Blood Flow Simulation for the Liver after a Virtual Right Lobe Hepatectomy

Harvey Ho[1], Keagan Sorrell[2], Adam Bartlett[3], and Peter Hunter[1]

[1] Bioengineering Institute, University of Auckland, New Zealand
{harvey.ho,p.hunter}@auckland.ac.nz
[2] Dept. of Mechanical Engineering, University of Auckland, Auckland, New Zealand
[3] Dept. of Surgery, University of Auckland, Auckland, New Zealand

Abstract. In this paper we present a hybrid 0D-3D modeling method to investigate the hepatic flow in a virtual right lobe hepatectomy (RLH), the surgical procedure for adult-to-adult living donor liver transplanation (LDLT). The 3D method is employed to simulate complex 3D flow in the portal vein, and the 0D model is used to study the systemic hepatic circulation. In particular, we quantify the flow velocity and wall shear stress (WSS) in the left portal vein which increase dramatically post-RLH, and also simulate the essential hepatic distribution features in a healthy adult pre- and post-procedure. We further predict the arterial flow in the remnant left liver, which would decrease due to a hepatic arterial buffer response (HABR) effect. Finally we discuss the physiological significance of these phenomena, and the potential of this hybrid modeling approach.

1 Introduction

Liver transplantation is the treatment of choice for patients with end-stage liver disease [1]. However, there is a huge and growing disparity between supply and demand for cadaveric liver donors. Some patients on the waitlist are delisted due to deteriorated condition or death while waiting for a cadaveric liver to become available. One solution to alleviate this problem is the living donor liver transplantation (LDLT), whereby a portion of a living donor's liver is resected and transplanted to a recipient. Fig. 1 illustrates a LDLT scenario. Fig. 1(a) shows a whole liver and its vascular systems, which include a portal venous (PV) tree and a hepatic arterial (HA) tree suppling blood to the liver, and a hepatic venous (HV) tree which drains the blood into the inferior vena cava (IVC). In a right lobe hepatectomy (RLH), the larger right lobe is harvested and transplanted to an adult recipient. The remnant left lobe, about 30-40% of total liver mass, is perfused by the left portal vein (LPV), left hepatic artery (LHA) and drained by the left hepatic vein (LHV).

It has been reported that dramatic hepatic flow alterations would occur in both donor and recipient after the procedure [2,3]. For instance, in the left lobe of the donor, which previously only receives about 30-40% of total portal flow,

N. Ayache et al. (Eds.): MICCAI 2012, Part III, LNCS 7512, pp. 525–532, 2012.

now receives the full portal inflow. Furthermore, the cardiac output after a lobectomy will increase [2]. This leads to an elevated total portal inflow immediately after the procedure. These dual effects would cause portal hyperperfusion, which actually is one of the major mechanisms driving liver regeneration following resection [3]. However, RLH carries with it the risk of donor mortality and mobidity. Therefore a good understanding of the perfusion pattern of the remnant liver is essential [2].

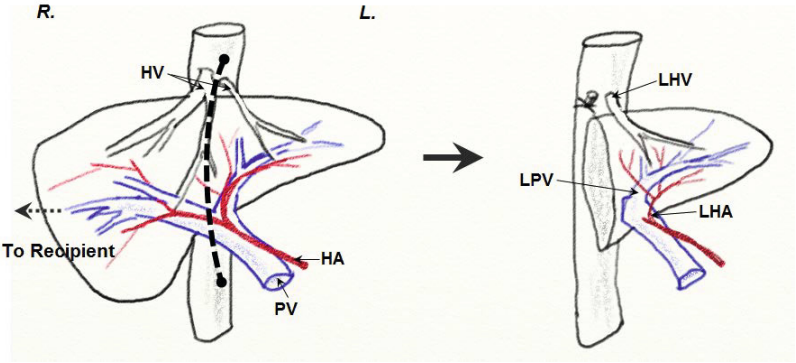

Fig. 1. Vascular anatomy of the liver: (a) the whole liver is supplied by a PV tree and a HA tree, and drained by a HV tree; (b) the remnant left liver, about 30-40% of total liver volume, is supplied by the l. HA and l. PV, and drained by l. HV. The bold broken curve represents the incision line. Abbreviations: HV - hepatic vein; HA - hepatic artery; PV - portal vein.

Three-dimensional (3D) flow in portal vein pre- and post-RLH was previously simulated by Ho *et al* [3]. They showed that increased portal flow and more complex flow streamlines occurred after the procedure, and speculated that this might be one of the main mechanisms that trigger a portal vein remodeling [3]. The systemic circulation pattern in the remnant liver, such as what would be the overall perfusion pattern, and how would arterial flow change with respect to increased PV flow, remain uninvestigated from a computational perspective.

In this work we propose a hybrid 0D-3D method to study hepatic flow from different perspectives, which could better prepare us to address these questions. We will reconstruct hepatic venous structures from a CT image, perform a virtual RLH, and simulate flow variations due to the virtual procedure. We will show the simulation results, and finally discuss the significance of this work.

2 Method

2.1 Medical Imaging and Vascular Construction

We studied the CT image (GE LightSpeed) of a male patient, who was admitted to the hospital due to a pathological condition (aneurysm) not relevant to the

liver. The spatial resolution of the image was $0.879 \times 0.879 \times 0.625$mm. The image, shown in Fig. 2(a), was used to visualize the portal and hepatic veins. Using a MIMICS software (Materialise, Leuven, Belgium) we segmented the liver and intrahepatic PV and HV trees. Also segmented are the superior mesenteric vein (SMV) and the splenic vein (SV), which merge into the PV (see Fig. 2b). To facilitate 3D flow simulation, the portal veins downstream the second generation were discarded because the image resolution was not high enough for us to conduct an accurate 3D vascular surface-reconstruction. A virtual incision line, indicated by the red line in Fig. 2(c), was assumed to occur at the right portal vein.

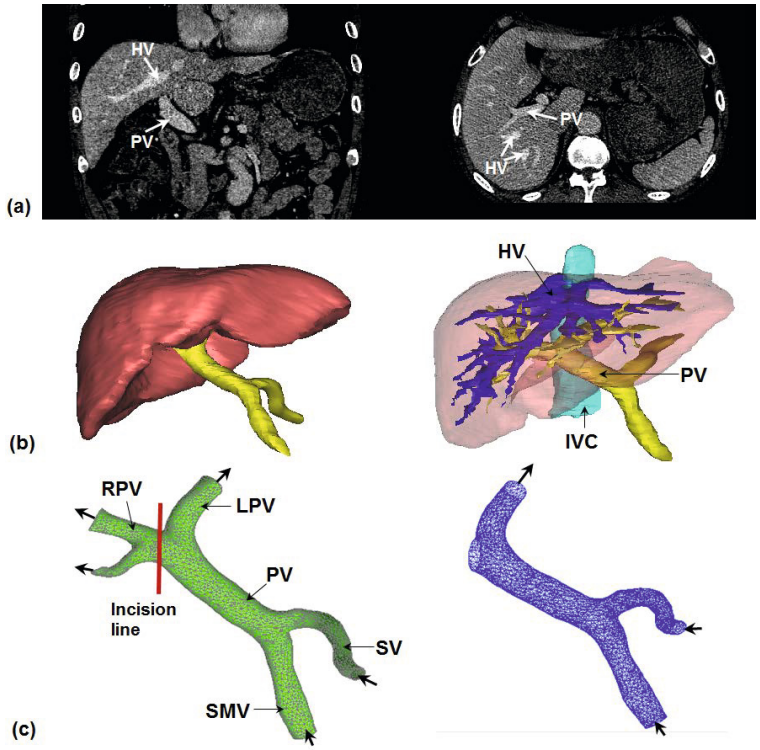

Fig. 2. Medical imaging and vascular construction: (a) front and axial view of the CT-image; (b) segmented PV and HV trees; (c) the portal vein is trimmed after the second generation. The red line indicates incision position and the bold arrows indicate flow directions.

The surface mesh of the PV, SMV and SV (see Fig. 2c) was imported into an ICEM software (ANSYS Inc.) for computational grid generation. The number of generated tetrahedral elements was about 160K.

2.2 Blood Flow Modeling

A hybrid 0D and 3D method was employed for blood flow modeling, whereby the 3D method was used for the simulation of complex 3D flow, and the 0D model for systemic circulation analysis, as briefed below.

3D Flow Simulation. The governing equations for blood flow in large arteries, the Navier Stokes equations, are expressed as:

$$\nabla \cdot \mathbf{v} = 0 \tag{1}$$

$$\rho(\frac{\partial \mathbf{v}}{\partial \mathbf{t}} + \mathbf{v} \cdot \nabla \mathbf{v}) = -\nabla p + \nabla \cdot \tau \tag{2}$$

where $\mathbf{v}$ and ρ represent the flow velocity and density of blood, respectively. p and τ represent the blood pressure and shear stress. The equations (1-2) were discretized over the computational grid of the portal system shown in Fig. 2(c), and were solved numerically using a finite volume based computational fluid dynamics solver, ANSYS CFX [4]. The portal flow was considered as steady, as revealed by ultrasonic measurements [3]. The inflow velocity boundary conditions, 20 cm/s and 30 cm/s, were prescribed at SV and SMV, respectively. These data were adopted from literature [2,3]. In addition, a zero pressure was imposed at the outlet(s) to allow free outflow.

0D Flow Simulation. For hepatic circulation models we follow the strategy of Debautt *et al* [5], who employed a dual source circuit to study hepatic perfusion. The difference between our model and that of [5] is that, instead of employing a large number of pi-filters for various PV, HV and HA generations, we simply used one pi-filter for each tree, therefore significantly simplified the circuit. The circuit, shown in Fig. 3, represents a basic hepatic circulation model. The direct current (DC) source in the circuit generates portal flow, whilst the pulsatile current (PC) source produces arterial flow. Note, that the law of mass conservation i.e. the hepatic inflow equals hepatic outflow ($F_{PV} + F_{HA} = F_{HV}$) is naturally obeyed in the circuit.

The parameters of the electronic components in a pi-filter (shown in Fig. 3b) are calculated based on a set of equations, e.g., [5]:

$$R_S = \frac{8\mu l}{\pi r^4} \tag{3}$$

$$L = \frac{1.33\rho l}{\pi r^2} \tag{4}$$

where μ is the viscosity of blood, l, r are the length and radius of blood vessel, respectively. The hepatic arterial resistance R_{HA} is a nonlinear element to simulate a hepatic arterial buffer response (HABR), the intrinsic regulating mechanism whereby the changes of hepatic arterial flow counteracts that of portal flow [6].

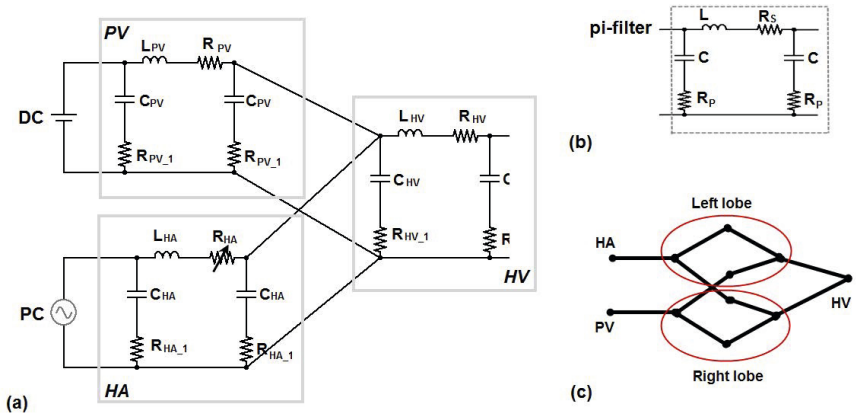

Fig. 3. Electrical analog circuits for hepatic circulation. (a) Basic model: the three pi-filters simulate flow in HA, HV and PV trees (each shown inside a gray rectangle); (b) a pi-filter; (c) the schema of the extended circuit accounts for the hepatic circulation to the left and right lobes. The parameter values of the electric components are shown in Table 1.

Table 1 lists the parameters for the electronic components in Fig. 3(a). Their values are based on the data in [5], and were fine-tuned after simulations.

Since the left and right lobes of the whole liver are perfused and drained independently, the basic electric circuit of Fig. 3(a) was expanded into a more complex circuit that differentiates the left and right lobes. The schema of this electric circuit is shown in Fig. 3(c). Note, that each segment in the circuit represents a pi-filter, and that the two lobes receive different portion (left: 40%, right: 60%) of total HA and PV flow, with each lobe drained by a single hepatic vein.

3 Results

3.1 3D Flow Alteration in the Portal Vein

The 3D flow simulation took about 30 minutes to complete on a desktop computer (Intel Core 2.4GHz). A variety of hemodynamic data were computed. Of particular interest are the flow velocity and the wall shear stress (WSS) pre- and post the virtual RLH procedure.

Fig. 4(a) visualizes flow streamlines along the flow path. It shows that the peak flow velocity in the LPV increased from 18cm/s to 46cm/s, as a result of receiving full portal flow. Consequently, the WSS in the LPV, shown in Fig. 4(b), was drastically elevated from merely 0.2Pa pre-RLH to 0.6Pa post-RLH. This agrees with the simulation of [3] which showed that WSS almost doubled post-RLH (from 0.4 Pa to 0.8 Pa). Also observable are the strong helical flows (indicated by slim arrows) in PV developed after the merging point of the SMV and SV.

Table 1. Parameters of Electronic components in Fig. 3(a)

Component	Whole organ	Unit
R_{HA}	1.5689e9 (nominal value)	$Pa \cdot s/m^3$
R_{HV}	1.3630e8	$Pa \cdot s/m^3$
R_{PV}	3.7807e7	$Pa \cdot s/m^3$
R_{HA_1}	1.562e10	$Pa \cdot s/m^3$
R_{HV_1}	1.40607e7	$Pa \cdot s/m^3$
R_{PV_1}	2.1054e8	$Pa \cdot s/m^3$
R_{IVC}	16.5e6	$Pa \cdot s/m^3$
C_{HA}	1.2803e-10	$m^3/Pa \cdot s$
C_{HV}	1.4224e-6	$m^3/Pa \cdot s$
C_{PV}	9.4995e-9	$m^3/Pa \cdot s$
L_{HA}	200e6	$Pa \cdot s^2/m^3$
L_{HV}	30e6	$Pa \cdot s^2/m^3$
L_{PV}	50e6	$Pa \cdot s^2/m^3$

This was not presented in [3] because that study placed the flow inlet after the SMV-SV junction. The physiological implications of the helical flows to PV wall remodeling remain to be investigated.

3.2 Hepatic Circulation in the Whole Liver and the Left Lobe

The portal vein pressure was assumed to be 6 mmHg at DC, and a pulsatile pressure varying between 80mmHg and 120mmHg was prescribed from the PC. The resulted flow rate waveforms of PV, HA and HV in the whole liver are plotted in Fig. 5(a). In particular, the total hepatic flow (F_{HV}) is about 1.45 L/min, i.e. approximately 30% of the cardiac output (∼5 L/min) in a healthy adult. The hepatic arterial flow, which is more pulsatile than the portal and hepatic venous flows, contributes about 400mL/min (or 33%≈1/3 of total hepatic flow volume) oxygenated blood to hepatic circulation, whilst the portal vein supplies the remaining 1,050 mL/min (or 67%≈ 2/3 of total volume) poorly-oxygenated yet nutrient-borne blood.

The above flow distribution represents the essential hepatic circulation features in a healthy adult, and was achieved by using the electric circuit of Fig. 3(a). We further analyzed the flow distribution into the left and right lobes using the extended circuit of Fig. 3(c). Fig. 5(b) shows the results: the flow rate in LPV is 1.05 L/min post-RLH, almost threefold of that pre-RLH (380 mL/min). This causes portal hyperperfusion (and high shear) in the LPV, as also revealed from 3D simulations. On the other hand, the left arterial flow decreases from 140 mL/min pre-RLH to 50 mL/min post-RLH. This surprising phenomenon is due to the HABR that was observed in partial liver grafts in recipients [7]. The presumed aim of this intrinsic mechanism is to keep the total hepatic circulation within a physiological range.

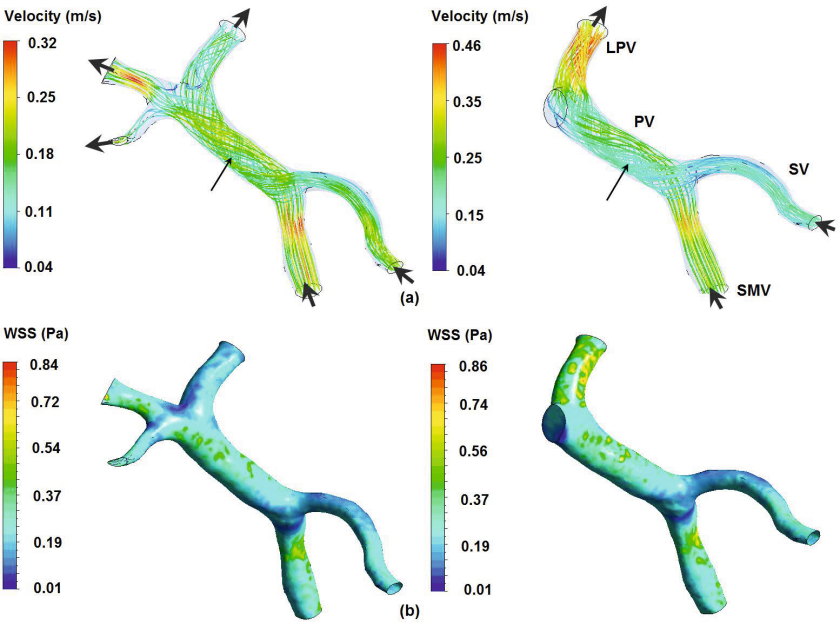

Fig. 4. Comparison of hemodynamic data pre- and post-RLH (a) flow streamline: helical flows are formed after the SMV and SV junction. The flow velocity increase in the LPV from 18cm/s to 46cm/s; (b) wall shear stress in the LPV is drastically increased, from merely 0.2Pa to 0.6Pa.

4 Discussion

Right lobe hepatectomy is the surgical method used in adult-to-adult LDLT [1]. Donor mortality and morbidity may occur due to multiple factors such as inadequate remnant liver mass, compromised hepatic circulation, etc. A comprehensive understanding of hepatic circulation in the remnant liver would aid biomedical and surgical research of this procedure. In this paper we used a hybrid 3D-0D method for the flow analysis of a virtual RLH. In particular, we simulated the essential flow distribution feature in the whole liver, and also in the remaining left lobe. This has never been performed previously, to our knowledge. Moreover, we made a physiological predication that hepatic arterial flow may decrease sharply in the liver remnant following RLH. This decrease, after verified through *in vivo* ultrasonic measurements, could be of significance. The possible implications of such a decrease are many, for example hepatic arterial thrombosis is a life-threatening disorder that is associated with liver dysfunction.

The presented models can be further extended to study more complex and clinically-related hepatic circulation problems. For instance, the pathological condition of the liver, e.g., cirrhosis, may be taken into the circulation model by altering the hepatic venous resistance and raising the portal pressure.

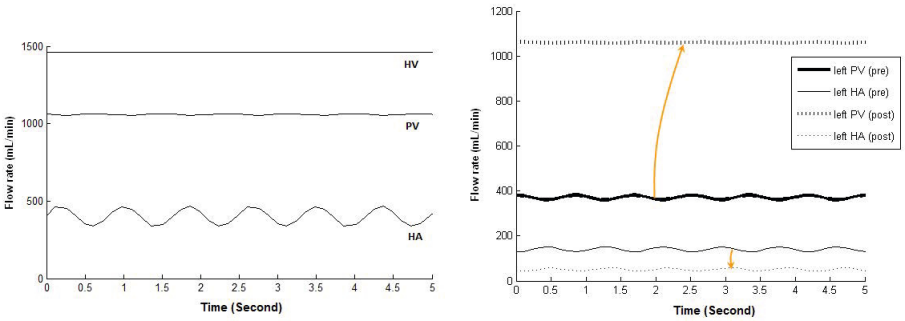

Fig. 5. (a) Flow rate in the HV, HA and PV in a whole liver: HA contributes 1/3 of total hepatic flow whilst PV contributes the rest; (b) LPV flow drastically increases but the LHA flow decreases due to the HABR effect

5 Conclusion

In this paper we simulated blood flow in a virtual right lobe hepactomy that was constructed from a 3D CT image. We showed the increased flow velocity and wall shear stress in portal vein, and reproduced the essential flow distribution features in the whole liver and the remnant left lobe.

References

1. Lo, C.M., Fan, S.T., Liu, C.L., Wei, W.I., Lo, R.J., Lai, C.L., Chan, J.K., Ng, I.O., Fung, A., Wong, J.: Adult-to-adult living donor liver transplantation using extended right lobe grafts. Annals of Surgery 226(3), 261–270 (1997)
2. Niemann, C.U., Roberts, J.P., Ascher, N.L., Yost, C.S.: Intraoperative hemodynamics and liver function in adulttoadult living liver donors. Liver Transplantation 8(12), 1126–1132 (2002)
3. Ho, C., Lin, R., Tsai, S., Hu, R., Liang, P., Sheu, T.W., Lee, P.: Simulation of portal hemodynamic changes in a donor after right hepatectomy. Journal of Biomechanical Engineering 132(4), 041002–041007 (2010)
4. ANSYS: ANSYS CFX-Solver, Release 10.0: Theory. ANSYS Europe Ltd. (2005)
5. Debbaut, C., Monbaliu, D., Casteleyn, C., Cornillie, P., Loo, D.V., Masschaele, B., Pirenne, J., Simoens, P., Hoorebeke, L.V., Segers, P.: From vascular corrosion cast to electrical analog model for the study of human liver hemodynamics and perfusion. IEEE Transactions on Biomedical Engineering 58(1), 25–35 (2011)
6. Lautt, W.W., Greenway, C.V.: Conceptual review of the hepatic vascular bed. Hepatology 7(5), 952–963 (1987)
7. Marcos, A., Olzinski, A., Ham, J., Fisher, R., Posner, M.: The interrelationship between portal and arterial blood flow after adult to adult living donor liver transplantation. Transplantation 70(12), 1697–1703 (2000)